Revista Mexicana de Física **43**, *No. 3 (1997) 436–450*

Surface of latex films imaged by atomic force microscopy

ELÍAS PÉREZ, PIERRE MARION, FLAVIO VÁZQUEZ,* MONIQUE SCHEER, THA PITH, MORAND LAMBLA, AND JACQUES LANG†

Institut Charles Sadron (CRM–EAHP), Strasbourg
6 rue Boussingault, 67083 Strasbourg Cédex, France

Recibido el 19 de junio de 1996; aceptado el 30 de octubre de 1996

ABSTRACT. Atomic force microscopy (AFM) has been used to image latex film surfaces in the standard contact mode (CM) and in the tapping mode (TM). The TM gives sharper images than the CM, but particle shapes have been observed with the TM which closely resemble to shapes predicted or described in the literature and which were artifacts due to damaged tips. Comparison between AFM and scanning electron microscope images of closed-packed latex particles, indicate that the hexagonal contour of the particles seen by AFM can be real, and is not simply due to the triangular or conical shape of the tip. Finally, particles coming from two different synthesis are shown. The one gave latex particles very monodisperse in size, and the other gave two populations of latex particles clearly seen by AFM. The smallest particles of the second synthesis could not be evidenced by quasielastic light scattering (QELS). Therefore, with QELS the second latex appeared monodisperse in size. This shows the advantage of AFM over QELS.

RESUMEN. Se ha recurrido a la microscopía de fuerza atómica (AFM) para obtener imágenes de superficies de películas de látex en el modo normal de contacto (CM) y en el modo oscilatorio (TM). El modo TM da imágenes más finas que el modo CM, pero se han observado con el primero formas de las partículas muy parecidas a las predichas o descritas en la literatura y las cuales eran artefactos debidos a puntas dañadas. Comparaciones entre AFM e imágenes de microscopía electrónica de barrido de partículas de látex empacadas, indican que el contorno hexagonal de las partículas vistas por AFM puede ser real, y no es debido simplemente a la forma triangular o cónica de la punta. Finalmente, imágenes de partículas provenientes de dos diferentes síntesis son mostradas. Una de las síntesis permitió la obtención de partículas de látex con una gran monodispersidad en tamaño, y la otra dio dos poblaciones de partículas de látex claramente visibles por AFM. Las partículas más pequeñas de la segunda síntesis no pudieron ser detectadas por dispersión cuasi-elástica de la luz (QELS). Además, mediciones de QELS muestran que el segundo látex es monodisperso en tamaño. Esto muestra las ventajas de la AFM respecto a la QELS.

PACS: 68.55.Jk; 68.65.+g

*Present address: UAEM, Facultad de Química, Departamento de polímeros, apartado postal A-20, 50000 Toluca, Edo. de México, Mexico.

†To whom correspondence should be addressed.

1. INTRODUCTION

Atomic force microscopy (AFM) was invented in 1986 by Binnig, Quate and Gerber [1], and has been used since then in many areas of science for the study of the topography of different types of surfaces, or to elucidate the structures of assemblies of organized molecules or the structure of individual molecules mainly in the field of biology. These studies have been mostly carried out on materials which are not electrically conductive and for which this microscopy technique is well appropriate.

The basic principle of AFM consists of a tip attached to a cantilever with the tip being in direct contact with the surface. The surface can be simply scanned under the tip and the deviation of the cantilever is then a measure of the topography of the surface. With this set-up the force exerted by the tip on the sample surface varies. The deflection of the cantilever can also be maintained constant by moving the sample surface up and down during scanning. In this case it is the movement of the sample which is a measure of the topography of the surface, and the force applied by the tip on the sample surface is constant. Moreover, the force of the tip acting on the sample can then be minimized in order to avoid as much as possible perturbation of the surface. This is particularly useful in the study of soft material.

Two modes of contact of the tip with the surface are now employed. In the first mode the tip stays constantly into contact with the surface. It is called the contact mode (CM). This mode has been the most currently used so far. In the second mode the tip oscillates as the surface is scanned under the tip. In this mode the tip interacts with the surface only periodically and the contact of the tip with the surface is considerably reduced (for more details see materials and methods). This mode, called the tapping mode (TM), is particularly appropriate to the study of soft material which can be easily destroyed as the tip rasters the surface. The tapping mode became recently commercially available, and one can guess that much work will be done in the future with this technique.

We have been involved in several studies on latex film using the CM in the past few years [2–5], and recently also with the TM. With the TM various new morphologies of the latex particles were imaged, which were not seen before when using the CM. Since the resolution with the TM was supposed to be much better than with the CM, it was natural to believe that the TM was displaying the real morphology of the particles. Moreover, many of these morphologies were analogue to morphologies predicted theoretically [6, 7]. They were in fact tip effects. One of the purpose of this work is therefore to point out some care that one must take when using the TM. Notice that several other works, besides ours, were done by AFM on latex films with the CM [8–15]. Apparently only one study, in this field, was undertaken with the TM [16], but it concerns isolated particles or clusters of latex particles rather then latex films.

We will first show some advantages of the TM over the CM using "good" tips. We will also compare images of latex films taken with AFM and scanning electron microscopy (SEM). This comparison is useful since the reality of the particle hexagonal contour seen by AFM has been contested. Next we will show tip effects. Finally, at the end of this paper we will briefly give an example which shows that AFM is a very convenient tool to appreciate the shape and polydispersity in size of latex particles which cannot be done by light scattering for instance, or which can be done by SEM but involves then a

more sophisticated film preparation. This is particularly useful to know at which stage of a latex synthesis modification to the operative conditions should be made to obtain monodisperse particles of a desired size.

The work presented here concerns latex films, but some of the conclusions are valid for other systems. All the films investigated are nascent films, *i.e.*, they were not brought at a temperature above T_g. The only special case concerns latex L2 (see below) who has a poly (butyl acrylate) core with a T_g much below the ambient temperature, but the shell [poly (methyl methacrylate)] has a T_g much above ambient temperature.

2. MATERIALS AND METHODS

2.1. LATEX SYNTHESIS

Five types of latexes were prepared for this study. In the following they are named L1 to L5. They were synthetized by free radical emulsion polymerization using $K_2S_2O_8$ as initiator. Latexes L1, L3, L4 and L5 were synthesized at the CRM and latex L2 at the EAHP, Strasbourg.

Latex L1 and L3 were synthesized in a batch polymerization without surfactant following the procedure described elsewhere [17]. For latex L1 the following amounts were used in our recipe: methyl methacrylate (MMA) (gift from EAHP), 8 ml; water, 100 ml; $NaHCO_3$ (Prolabo), 0.086 g; $K_2S_2O_8$ (Aldrich), 0.062 g; 24 h at 80°C. The same recipe was used for latex L3, except that MMA was replaced by a mixture of MMA (5.2 ml) and butyl methacrylate (BMA, Aldrich) (2.8 ml).

Latex L2 was synthesized in a semicontinuous polymerization. A preemulsion, P1, containing the monomer [butyl acrylate (BA, Atochem), 199 g], a crosslinking agent [ethylene glycol dimethacrylate (EGDMA, Aldrich), 1 g], a buffer ($NaHCO_3$, 0.585 g), an ionic surfactant [ammonium nonylphenol poly (glycol ether) sulfate containing 25 ethylene oxide units (NPGE, Seppic), 5.64 g] and water, (118.8 g), was added, under starving conditions, to 151.5 g aqueous solution of NPGE (0.05 g) and $K_2S_2O_8$ (0.348 g, Aldrich). Preemulsion P1 was destined to form the core of the particles. Next, a preemulsion P2 was introduced to the reactor, also under starving conditions. Preemulsion P2 was destined to form the shell of the particles. It had the same composition that preemulsion P1, except that BA was replaced by MMA (Aldrich) and that it contained a transfer agent (tert-dodecylmercaptan, 0.67 g, Aldrich) not present in preemulsion PI. An aqueous solution of $K_2S_2O_8$ (0.81 g in 50 g total solution) was added to the reactor during introduction of preemulsions P1 and P2. A detailed description of the experimental set-up for latex L2 synthesis will be given elsewhere [18].

Latex 14 and 15 were synthesized by a semicontinuous polymerization following the procedure described by Zhao *et al.* [19]. A latex seed was first prepared and next the rest of the components were slowly added in two steps. For latex L4 the following amounts were used in the seed: BMA, 2.91 g; water, 45 g; $NaHCO_3$ (Prolabo), 0.0816 g; $K_2S_2O_8$ (Aldrich), 0.0428 g; sodium dodecyl sulfate (SDS, Touzart and Matignon), 0.0305 g. For the synthesis of the core, BMA (15.7 g) was added to the seed (step 1), and for the synthesis of the shell a mixture of three monomers [BMA, 1.2 g; BA, 1.4 g; and a third monomer MN (see below), 4 g] was next added to the emulsion (step 2). A solution

TABLE I. Characteristics of the latexes used in the present study

Latex	Structure (Wt%)	Chemical Composition	T_g (°C)	Particle Diameter (nm)	
				AFM	QELS
L1	Homogeneous 100	Poly (MMA)	110	315	324
L2	Core-Shell 50-50	Poly (BA)-Poly (MMA) 0.25% of EGDMA	−50/110	210	180
L3	Homogeneous 100	Copoly (BMA-MMA)	100	270	282
L4	Core-Shell 74–26	Poly (BMA)- Copoly (BMA-BA-MN)	34/34	50–230	240
L5	Core-Shell 74–26	Poly (BMA)- Copoly (BMA-BA-MN)	34/34	260	300

containing water (20 g), $K_2S_2O_8$ (0.0361 g), and SDS (0.37 g) was independently added to the reactor during step 1 and 2. The overall time for the reaction was 20 h (seed: 1 h; step 1 and 2: 8 h; emulsion let under gently stirring: 11 h), and the temperature 80°C. Latex L5 was synthesized exactly as latex L4 except that only 0.28 g of SDS was used in the aqueous solution added during step 1 and 2, instead of 0.37 g in case of latex L4.

The nature of the third monomer which partly composes the shell of the particles in latex L4 and L5 cannot be given yet for industrial reasons. However the knowledge of the chemical structure of this monomer will have no incidence on the interpretation of the results reported here. A detailed description of the synthesis of latex L4 and L5 will be given in the future. Table I gives some characteristics of the latexes used in the present study.

2.2. FILM PREPARATION FOR AFM IMAGING

Solid deposits of thin layers were prepared by pouring a few drops of latex dispersion onto freshly cleaved mica plates, 10×30 mm^2 in size, and allowing to dry at ambient air, *i.e.*, at a temperature below the polymer glass transition temperature T_g except for latex L2 (core made of PBA), for at least four hours. Once the film was dry a small region, 8×8 mm^2 in size, was selected to be imaged. This region was selected to avoid the "last drop" region [5] where the last part of water evaporates and may contain different kinds of impurities coming either from the dispersion (surfactant) or from outside (dust). Dry films were about 10 to 100 μm thick. For particles with a diameter of 200 nm these thicknesses correspond, at least, to 50 to 500 layers of particles. The 8×8 mm^2 mica plate was next placed on the top of the piezoelectric translator, and the surface of the dry film imaged either by CM or by TM.

2.3. ATOMIC FORCE MICROSCOPY

The model used was a Nanoscope III from Digital Instruments (Santa Barbara, CA) equipped with a modified version of Nikon's model MM-11U optical microscope which allows a prelocalization of the area of interest. This prelocalization allowed us to avoid the contact of the tip with cracks which form often at the film surface as the dispersion dries, and which could damage or even break the tip during scanning. The piezoelectric translator was able to scan a maximum area of 12×12 μm^2. Both with the CM and the TM scans were operated in the height mode, which means that the force exerted on the film by the cantilever tip during the scan was kept constant by varying the height of the sample relative to the tip through an electronic feedback loop. The scan rate was 1 Hz in both modes. With the CM the spring constant of the cantilever was 0.58 $N \cdot m^{-1}$. With the TM the spring constant of the cantilever was much higher (around 50 $N \cdot m^{-1}$) but with this mode the tip stays only for a very short period of time in contact with the surface (tip oscillation frequency around 370 Hz), and thus the mean lateral force exerted by the tip on the surface is considerably reduced compared to the situation in constant contact mode. The oscillation of the tip is produced by a small piezoelectric translator located below the substrate to which the cantilever tip is attached. The cantilever and the tip (NanoProbes$^{(TM)}$) used in the CM are made of silicon nitride (Si_3N_4) and in the TM of silicon. The quality of the Si_3N_4 tips was checked by imaging a mica surface at the atomic scale, and that of the silicon tips by imaging a latex surface of polydisperse spherical particles whose topography was previously determined from several investigations done with new TM tips (see below). Check of the quality of the tips was made before and after imaging each latex surface studied. No filter treatment was done to the image and all measurements were performed in ambient air.

2.4. SCANNING ELECTRON MICROSCOPY

SEM experiments were performed with a Hitachi 2300S operating at 25 KV and having a resolution of 4.5 nm. The preparation of the samples was the same as the one used for AFM imaging (see above), except that after air drying the films were coated, under 0.05 mbar vacuum pressure, with a thin layer (8 nm) of gold. The reduced pressure and the coating had no effect on the size and shape of the particles, which were found identical to those measured by AFM. They have also no effect on the defects observed at the surface of particles L2. Indeed, these defects appeared similar on the SEM and AFM images (see below comparison between Figs. 3 and 2B), the only difference being that with the SEM the defects appear smoother, and small defects are probably not apparent, compared to TM AFM. However basically the same defect are detected with both techniques. Finally, the thickness of the coating was small compared to the size of the particles (diameter between 200 and 320 nm, see Table I), and had no dramatic effect on the contour of the particles discussed below.

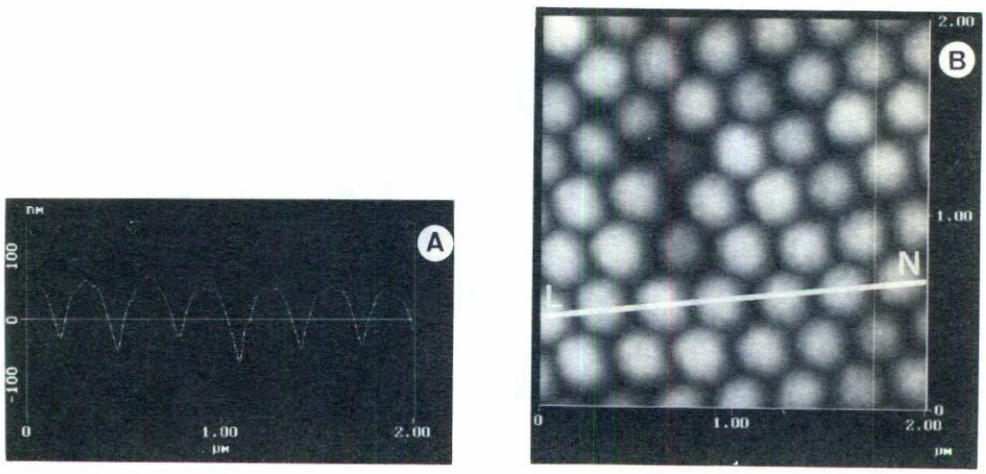

FIGURE 1. AFM height profile (A) and top view (B) of a film of latex L1. The height profile is taken along the LN-line drawn on the top view. The image has been taken with the standard CM.

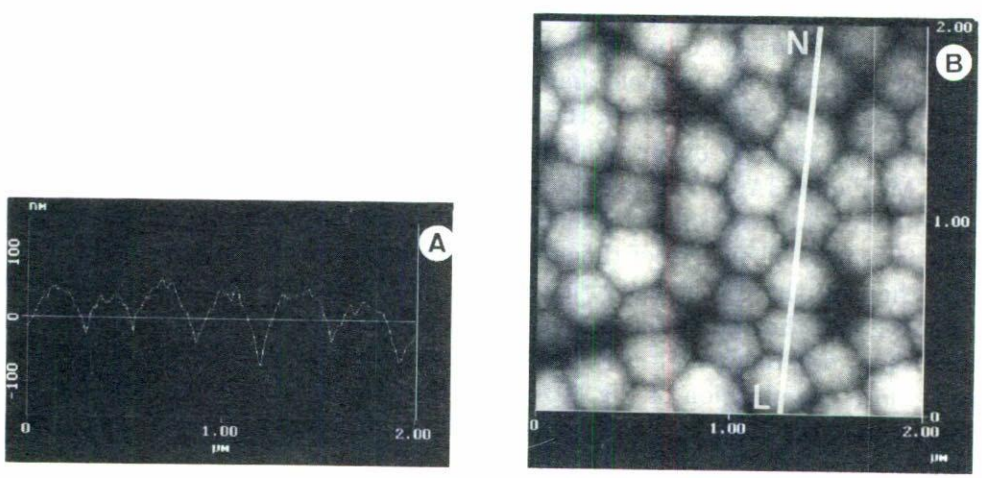

FIGURE 2. AFM height profile (A) and top view (B) of a film of latex L1. The height profile is taken along the LN-line drawn on the top view. The image has been taken with the TM.

3. RESULTS AND DISCUSSION

3.1. COMPARISON BETWEEN CM AND TM IMAGES

Figures 1 and 2 show top views of the surface of latex L1 imaged with the CM and the TM, respectively. On both images the latex particles form well known hexagonal close—pack (hcp) domains [2, 9] which characterize the face-centered—cubic (fcc) packing of the particles deformed into almost perfect rhombic dodecahedra in the interior of the film [17, 20, 21]. As it will be seen in the following the extent of these domains depends very much on the polydispersity in size of the particles. The important feature in Figs. 1 and 2 is that the particle surface is not smooth and this is better seen with the TM than

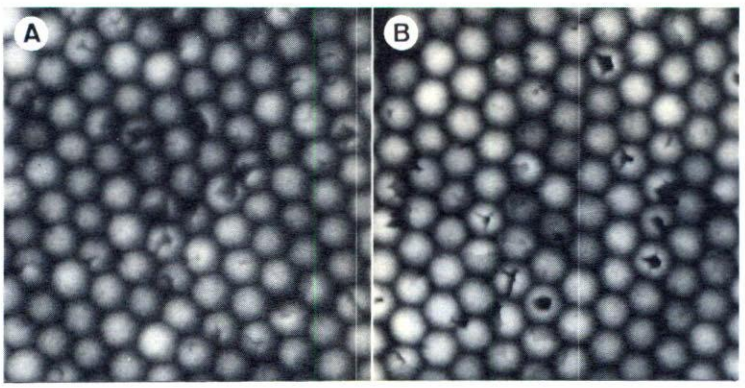

FIGURE 3. AFM top views of a film of latex L2 taken with the standard CM (A) and with the TM (B).

with the CM. Irregularities at the particle surface are clearly visible on the z-axis profiles shown in Figs. 1 and 2. These profiles are taken along the lines depicted on the x-y top views. The irregularities are better resolved in the TM profile than in the CM profile. However, as expected, the particle diameters, calculated with the Nanoscope software, are exactly the same (315 nm) with the two modes.

Figure 3 gives another example of the better resolution obtained with the TM than with the CM. Figure 3A and 3B are top views of the film surface of latex L2 imaged with the CM and the TM, respectively. One sees that many particles are broken or present a hole in their center. The edges of the cracks or holes are much sharper on the TM image (Fig. 3B) than on the CM image (Fig. 3A). In fact with the CM these defects appear rather smooth and they do not seem to go so deep inside the particles than with the TM. Of course these differences can also be clearly seen on the z-profiles (not shown here). Moreover, close examination of Fig. 3B shows that the shell is partly missing for some particles, or that the shell is slightly detached from the core of the particle. These last observations are hardly visible in Fig. 3A.

It is clear that images of Figs. 1B and 2B (latex L1) do not correspond to the same area of the film surface. This is also true for images of Figs. 3A and 3B (latex L2). It is, indeed, very difficult to scan exactly the same surface area, with our AFM, as one moves from one mode to the other. Therefore, it can be argued that the differences observed between images 1B and 2B, and 3A and 3B, are due to differences in the surface itself. However, many different areas of the film were scanned for both latexes; the TM always gave sharper images than the CM.

Note that the so called peak-to-valley distance, d [2, 3, 10], measured along height profile of aligned close packed particles is found generally larger with the TM than with the CM (we have found a factor of two for particles having a diameter of about 200 nm). This is a trivial tip effect due to the fact that the TM tip is longer and thinner than the CM tip. This also explains why the TM images are sharper than the CM images.

Figures 2 and 3 show very different structures of the latex particles revealed by AFM. In Fig. 2 the particles present a granulous surface (raspberry-like particles), whereas holes

and partly destroyed shells are seen for the particles in Fig. 3. Several sample preparations have led to the same observations. Some speculative explanations can be given for the structure found for the particles.

The particles in Fig. 2 are made of PMMA. Due to the solubility of MMA in water, homogeneous nucleation in the water phase occurs and the PMMA particles are partly build up by adsorption of oligomeric chains or primary particles [22]. Apparently these primary particles may give to the PMMA particle surface the granulous aspect seen by AFM. Moreover, the synthesis has been carried out at 80°C, *i.e.*, below the PMMA T_g which is equal to 110°C. This temperature is too high to allow a complete reorganization of the polymer chains inside the particles during synthesis, and thus to minimization of the interfacial tension between the particles and the surrounding water phase which would lead to the formation of smooth spherical particle surfaces.

The images in Fig. 3 show PBA-PMMA core-shell particles. In this case the particles are constituted from a very soft core ($T_g = -50$°C) and a hard shell ($T_g = 110$°C). The theoretical shell thickness is about 20 nm (it can be calculated from the recipe of latex L2 synthesis given in Sect. 2.1.). Analysis of the image in Fig. 3B made with the AFM software, indicates that the thickness of the shell, which is apparent for some particles where the shell is partly broken or missing, is comprised between 5 and 30 nm. These values are compatible with the theoretical value since a very regular shell is probably difficult to synthesized, and an unique value of the shell thickness along the particle surfaces was not expected to be found. However it is not possible, from our experiments, to know if the hole in the particles or the broken shell are formed during synthesis or during film drying.

3.2. Comparison between AFM and SEM images

Figure 4 shows SEM images of films of latex L1 (Fig. 4A), L2 (Fig. 4B), and L5 (Fig. 4C). Comparison of Figs. 2 and 4A shows that a much better resolution is obtained by TM AFM than by SEM. On the SEM image the particles present a smooth surface, whereas on the TM AFM image the surface appear irregular. On the other hand, most of the defects observed in Fig. 3B (TM AFM) are also apparent on the SEM image in Fig. 4B. Cracks are clearly visible and close examination of Fig. 4B also shows that part of the shell of some particles is missing. Thus the AFM and the SEM images give qualitatively the same information, but the AFM software allows a quantitative determination of the size of the defects which is out of the scope of this work.

Another comment on the SEM images concerns the overall arrangement of the particles at the film surface. It has been shown [23] that the hexagonal contour of the latex particles observed by AFM at the surface of latex films may result from the tip shape which gives an apparent hexagonal contour to particles which, in fact, are spherical (see Fig. 13a in Ref. 23). One can therefore wonder whether the hexagonal contour of latex particles seen usually by AFM on latex film surface is real. It is certainly true that the pyramidal or conic shape of the tip can modify the topography of the real latex film surface, chiefly for particles with a size close to the size of the apex of the tip, which seems to lie between 20 to 50 nm for CM tips [23]. This is perhaps partly the reason why, as said above, sharper images are obtained with the TM (TM tips are apparently

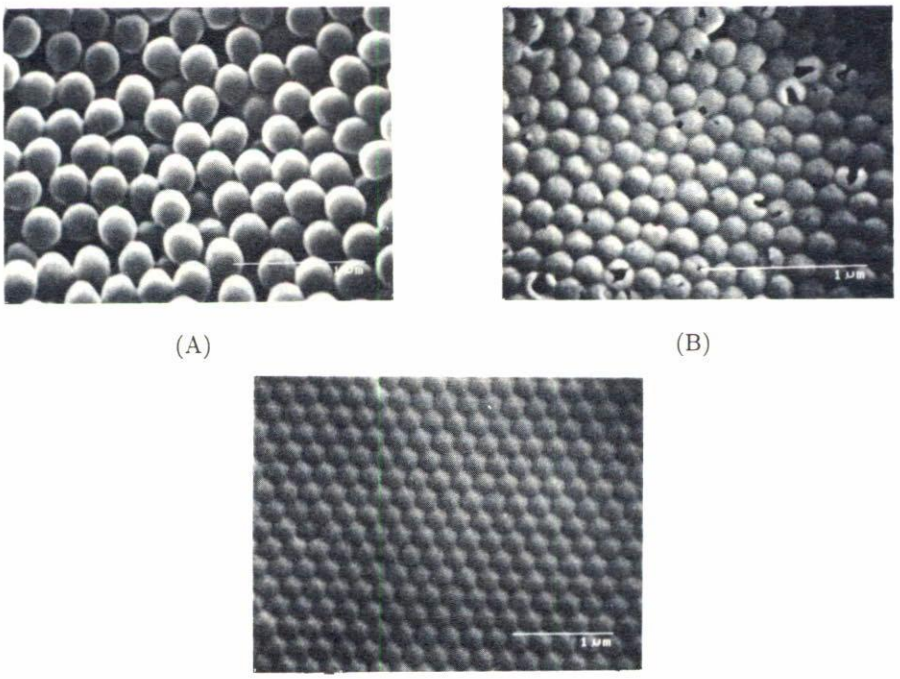

(A) (B)

(C)

FIGURE 4. SEM views of films of latex L1 (A), L2 (B) and L5 (C).

thinner) than with the CM (compare for instance Figs. 3A and 3B). However one must not forget that in most cases latex particles are deformed during drying of latex film due to capillary forces, and form, as said above, fcc packing of rhombic dodecahedra in the dry film [17]. Due to this deformation the particles at the film surface are hexagonally packed and present a hexagonal contour. Hexagonal contour of the particles have already be seen on surface film replica imaged by transmission electron microscopy in the early eighties [24]. The hexagonal contour of the particles is also seen in Figs. 4B and 4C, obtained by SEM. There is therefore no doubt that the hexagonal contour of the particles seen by AFM for the same films can be real, even thought the peak-to-valley distances [2, 3, 10] (not reported here) may be affected by the tip size and shape. Note also the close analogy (particle hexagonal packing and contour) between the images taken by SEM (Fig. 4C) and by AFM (Fig. 8B which will be discussed later in this paper). Therefore, nice simulations as those done with non-deformed spheres into contact [23] should also be done with hexagonally packed particles.

3.3. MISLEADING TM IMAGES

With the previous examples we have shown some advantages of the TM over the CM for imaging latex films. We will now show that the TM presents also some risks of error. Indeed, the TM tips are much more brittle than the CM tips. In our study of latex

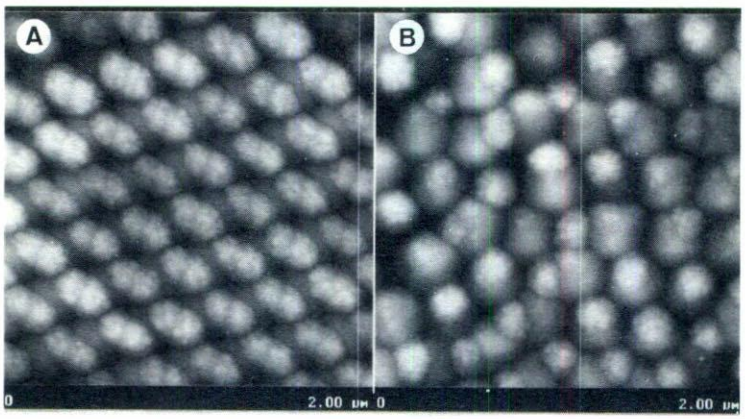

FIGURE 5. AFM top views of the surface of a film of latex L1 obtained with the TM. Images A and B have been obtained using two different damaged tips. The image of the particles in A and B are not real, and depend on the geometry of the damage done to the tip, as discussed in the text. The real size and shape of particles L1 are shown in Figure 2B.

film topography we have gotten a great number of TM images which appeared later to be artifacts due to broken tips. The main reason why these images were misleading is that they showed particles with a shape similar to shapes predicted from thermodynamic analysis [6, 25] or seen by optical and electron microscopy [7] for other latexes, as for instance symmetric or asymmetric doublets and ice-cream cone like particles. Although the present work is focused on latex, it is obvious that artifacts due to broken tips can also occur in the study of other surfaces. Note that other types of difficulty in the use of AFM [26] and scanning tunneling microscopy [27] have been mentioned in the literature.

It must be said here that the circumstances under which tips break are often difficult to determine and even more difficult to bring under control. Of course damage to the TM tips can be done by slightly touching the sample surface with the tip, but this can be avoided by the operator. From our experience the apex of the tip can also be damaged simply during scanning under normal working conditions. If this happens the operator may not be conscious of the damage caused to the tip and this can have dramatic consequences on the image and its interpretation.

Figure 5 presents two images of a film prepared with the latex L1. Both images are very different from the one shown in Fig. 2 in spite of the fact that they show the same surface imaged with the same mode, the TM. One could think that the particles in Fig. 5B are real since for instance polystyrene particles with an asymmetric shape have indeed been observed by optical photomicrography and SEM [7]. However, from our test (see below) we know that the good image is given in Fig. 2 and that the images in Fig. 5 result from an irregular shape of the tip. This shape is not known but could be obtained from a "deconvolution" calculation. Indeed, the structure of the particles in Fig. 5 results from the "convolution" of the real particle shape by the shape of the tip. However such a calculation would not be useful in practice. Even thought one uses well calibrated particles to determine the tip shape, one could not take real advantage of knowing it since tips are so brittle that their shape can change, as said above, just by

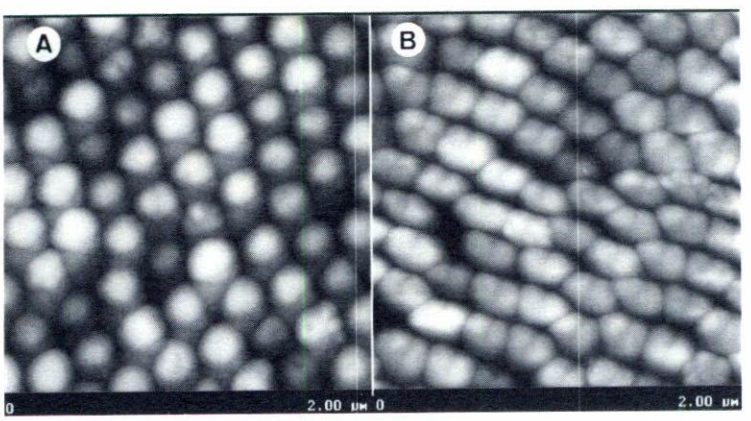

FIGURE 6. AFM top views of the surface of a film of latex L3 obtained with the TM. Images A and B have been obtained using two different damaged tips. The image of the particles in A and B are not real, and depend on the geometry of the damage done to the tip, as discussed in the text. In reality particles L3 are spherical (image not shown).

touching the surface or even during scanning. We believe that the best thing to do, in order to trust the TM images, is to check the quality of the tip before and after each surface imaging.

Our test was to image the surface of a known latex film topography containing small (diameter 80 nm) and large (diameter 210 nm) spherical particles (for instance as those shown below in Fig. 8A) before and after imaging each new sample. This was done throughout this work. Using this procedure we have been able to distinguish between "good" and "bad" or "wrong" images. The two "wrong" images in Fig. 5 are very different. They have been obtained with tips of different unknown shapes. Fig. 5A represents particles regularly oriented but formed from two different parts, one with a smooth surface and the other with a very granulous one. The particles in Fig. 5B seem much more realistic and can be interpreted as made of asymmetric doublets or representing a latex in which a second nucleation has taken place during synthesis. However, as said above, from the test of the tip quality we know that both images in Figs. 5A and 5B are "wrong". In fact the synthesis has led to the formation of rather monodisperse spherical particles (Fig. 2).

Figures 6A and 6B are for latex particles made of statistical BMA-MMA copolymers. On both images the particles appear to be composed of two parts just like if phase separation would has occurred in each particle. In Fig. 6A the particles have an ice—cream like structure and in Fig. 6B a preanut like structure. However we know from our test that these particle shapes are due to broken tips.

Formation of the images presenting double like particles as those shown in Fig. 6 can be easily understood if one assumes that the tip is ended by two apices separated by a distance close to the particle size. Each particle is then probed twice during scanning. This appears possible if one compares the dimensions of the tip with the dimension of the particles.

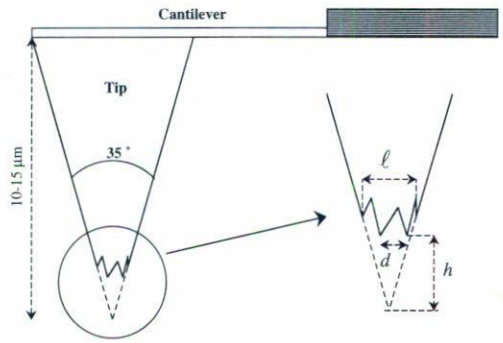

FIGURE 7. Schematic representation of the geometry assumed for a damaged TM tip. This geometry explains the particle shapes observed in Figs. 5 and 6.

The tips used in this work have a length comprises between 10 to 15 μm, and an interior cone angle close to 35° (see Fig. 7). The thickness of the tips at half high is therefore comprised between 3.2 and 4.7 μm which is a distance much larger than the diameter (between 200 and 310 nm, see Table I) of the particles investigated here. Thus, a small damage at the end of the tip, as shown in Fig. 7, can give rise to the formation of a double tip separated by a distance equal to a particle radius. In Fig. 7, d is the distance between the two extremities of the double tip. The distance d is supposed to be parallel to the cantilever plane. The distance l has been taken arbitrarily equal to $2 \times d$. If one assumes that d is equal to 125 nm (value of the radius of latex L3) then h, the distance between the extremity of the double tip and the apex of the original undamaged tip, is equal to 0.4 μm. This value represents only 4 to 2.7% of the original tip length. This elementary calculation shows that it is not unrealistic that a double tip forms at the extreme end of a tip, *i.e.*, without a large overall size modification of the tip. Thus, if such a double tip is employed to image a latex surface, particles with two hemispheres will be observed. In Fig. 6 the long axis of the apparent particles is not aligned along the x-axis. This is due to the fact that the direction of d is not parallel to the x-axis. However alignment of the double particles along the x-axis can be obtained by rotation of the x-scan relatively to the tip.

3.4. EFFECT OF SURFACTANT CONCENTRATION ON PARTICLE SIZE POLYDISPERSITY

In their recent work Sommer *et al.* [16] have used the AFM technique to follow the shell formation of PBA/PMMA core-shell latexes particles, upon progressive increase of the PMMA volume fraction. AFM images reveal that at low PMMA coverage, PMMA forms microbeads whose size increases with PMMA content to form particles with a raspberry-like structure, at a PBA/PMMA weight ratio equal to 80/20. At a weight ratio of 70/30 distinct beads are no longer observed, and at a 50/50 weight ratio the particles form an orange-like structure, which indicates an increasingly uniform coverage of the PBA core by the PMMA shell. This last result is in agreement with the image of PBA/PMMA (50/50 weight ratio) latex film surface shown in Fig. 3B, which indicates that the particles surface is rather smooth. However the presence of holes, cracks and defects in the shells

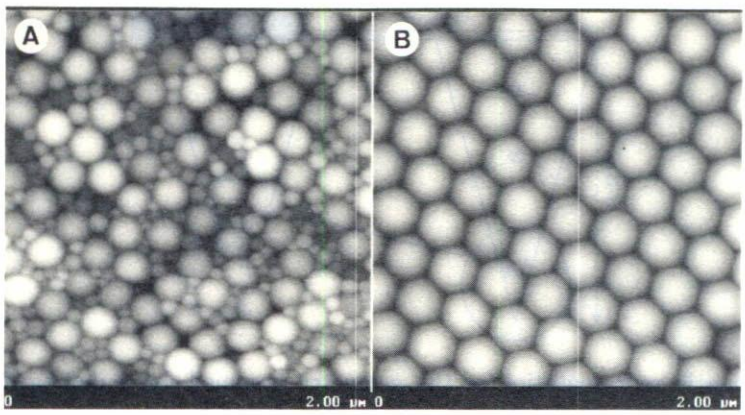

FIGURE 8. AFM top views of a film of latex L4 (A) and L5 (B) taken with the TM.

seen on the particles in Fig. 3B which were not observed for the latex particles by Sommer *et al.*, is probably due to differences in the latex synthesis conditions and in particular in differences in the nature and concentration of the cross linking and transfer agents used.

We are also using currently AFM to follow latex particle growth during emulsion polymerization, by measuring the size of the particles in the seed and after each other polymerization step, for example the size of the core and of the final core-shell particles. These measurements allow to calculate the concentration of particles in the emulsion in the course of the synthesis and therefore to check if the number of particles formed in the seed did stay constant during polymerization. We illustrate here the helpful use of AFM in latex synthesis with an example. Figs. 8A and 8B represent images of the surface of dry films made with latex L4 and L5, respectively. Both latexes have been obtained from a seeded semicontinuous emulsion polymerization, under the same conditions with only one exception: during the slow addition step (see latex preparation section) the amount of SDS introduce into the reactor was decreased by 24%, in going from the synthesis of latex L4 to that of latex L5. One sees (Fig. 8A) that in latex L4 two populations of particles have been formed, which indicates that a second nucleation has occurred during synthesis. This second nucleation has taken place during the slow addition of the reactants following seed formation. Indeed, decrease of the amount of SDS in latex L5 leads to particles perfectly monodisperse in size (Fig. 8B). Thus, the excess of surfactant in the synthesis of latex L4 has initiated a second nucleation. It must be noticed that quasielastic light scattering (QELS) experiments, made on latex L4 and L5, was not able to evidence the small particles in the dispersion of latex L4 and both latex dispersions L4 and L5 appeared to be composed of a distribution of identical large particles. This is due to the fact that the intensity of scattered light is much more sensitive to the large particles since it varies, in first approximation, with the particle diameter at the power six.

Another comment can be made concerning the images shown in Fig. 8B. Note first that the z scale representation on an AFM image is achieved by using a color scale, which is gray on our images. Darker is the color lower is the z value, and thus a same gray color

corresponds to a same height. Thus in Fig. 8B the film surface appears surprisingly flat and stays flat at a much larger scale than $2 \times 2\ \mu m^2$. At least three reasons can account for this observation. The great uniformity in size of the L5 latex particles, the minimization of the total surface energy at the latex film/air interface, as mentioned elsewhere [12], and an optimization of the surfactant concentration in the dispersion which, as discussed in other studies [2, 3], tends to reduce the formation of flocs during film drying and to increase particle ordering and packing inside the film and at the film surface. If one assumes that all the surfactant molecules are used to cover the latex particles in the dispersion of latex L5, then the surface area occupied by a surfactant molecule at the latex particle surface is equal to 80 $Å^2$. This value is close to the theoretical value of the surface occupied by an extended SDS molecule, which is about 100 $Å^2$. Thus, the surfactant concentration used in the synthesis of latex L5 is very close from the optimal surfactant concentration required to form a film with well ordered and packed latex particles [2, 3].

4. Conclusion

The main purpose of this paper was to point out that the tapping mode AFM can easily give wrong images of latex particles. The apparent shape of these particles resemble very much to shapes predicted on thermodynamics basis or seen by electron microscopy for other latexes. However, their real shape is different, and in general more simple than the shape shown by these wrong AFM images. Misleading AFM images come from damaged tip and can be avoided if one takes care to check the quality of the tip before and after each study. This can easily be done by imaging surfaces of well known topography. We have also shown that, in good working conditions, the tapping mode gives sharper images of latex particles in latex films than the contact mode, as shown elsewhere for individual latex particles [16]. Comparison between AFM images and SEM pictures of the same latex film surface of close-packed latex particles indicates that the hexagonal contour of the latex particles seen on the AFM images can be real and probably not simply simulated by the triangular or conical shape of the tip, as this might be thought from examination of apparent images of close-packed hard spheres obtained by other authors from simulation of particle contour which takes into account the shape of the tip [23]. The use of AFM in the check of latex synthesis has been illustrated by an example in which the surfactant concentration has been varied from one latex synthesis to another. In one case two latex populations, which could not be evidenced by QELS, are clearly visible on the AFM images. In the other case one observes very monodisperse latex particles.

Thus, because of its essentially non-destructive operative mode (especially when using the tapping mode) and the relatively easy sample preparation compared, for example, to sample preparation for electron microscopy measurements, AFM appears here again as being an useful tool to check the particles size and polydispersity in the course of a latex synthesis, and to have a good estimation of the quality of ordering and packing of latex particles at dry film surfaces. This study shows also that the use of tip presenting higher strength will increase the reliability of the images taken by AFM.

ACKNOWLEDGMENTS

The authors thank Sabine Graff (Institut Charles Sadron) for the SEM experiments. E.P. thanks the Mexican and French government for their financial support granted through the SFERE-CONACyT program.

REFERENCES

1. G. Binnig, C.F. Quate, and Ch. Gerber, *Phys. Rev. Lett.* **56** (1986) 930.
2. D. Juhué and J. Lang, *Langmuir* **9** (1993) 792.
3. D. Juhué and J. Lang, *Colloids and Surfaces A* **87** (1994) 177.
4. D. Juhué and J. Lang, *Double Liaison-Physique et Chimie des Peintures et Adhésifs* **464-465** (1994) 3.
5. D. Juhué, Y. Wang, J. Lang, O.M Leung, M.C. Goh, and M.A. Winnik, *J. Polym. Sci. Part B: Polymer Physics* **33** (1995) 1123.
6. D.C. Sundberg, A.P. Casassa, J. Pantazopoulos, M.R. Muscato, B. Kronberg, and J. Berg, *J. Appl. Polym. Sci.* **41** (1990) 1425.
7. J.W. Vanderhoff, H.R. Sheu, and M.S. El-Aasser, in: *Scientific Methods for the Study of Polymer Colloids and their Applications*, edited by F. Candau and R.H. Ottewill (Kluwer Academic Publishers, Dordrecht, 1990), p. 529, and references therein.
8. Y. Li and S.M. Lindsay, *Rev. Sci. Instrum.* **62** (1991) 2630.
9. Y. Wang, D. Juhué, M.A. Winnik, O.M. Leung, and M.C. Goh, *Langmuir* **8** (1992) 760.
10. M.C. Goh, D. Juhué, O.M. Leung, Y. Wang, and M.A. Winnik, *Langmuir* **9** (1993) 1319.
11. V. Granier, A. Sartre, and M. Joanicot, *J. Adhesion* **42** (1993) 255.
12. H.J. Butt, R. Kuropka, and B. Christensen, *Colloid Polym. Sci.* **272** (1994) 1218.
13. L. Nick, R. Lämmel, and J. Fuhrmann, *Chem. Eng. Technol.* **18** (1995) 310.
14. V. Granier and A. Sartre, *Langmuir* **11** (1995) 2179.
15. F. Lin and D.J. Meier, *Langmuir* **11** (1995) 2726.
16. F. Sommer, Tran Minh Duc, R. Pirri, G. Meunier and C. Quet, *Langmuir* **11** (1995) 440.
17. Y. Wang, A. Kats, D. Juhué, M.A. Winnik, R.R. Shivers, and C.J. Dinsdale, *Langmuir* **8** (1992) 1435.
18. F. Vázquez, T. Pith, and M. Lambla, to be published.
19. C.L. Zhao, Y. Wang, Z. Hrushka, and M.A. Winnik, *Macromolecules* **23** (1990) 4082.
20. B.J. Roulstone, M.C. Wilkinson, J. Hearn, and A.J. Wilson, *Polym. Int.* **24** (1991) 87.
21. Y. Chevalier, C. Pichot, C. Graillat, M. Joanicot, K. Wong, J. Maquet, P. Lindner, and B. Cabane, *Colloid Polym. Sci.* **270** (1992) 806.
22. M. Ballauf, *Macromol. Symp.* **87** (1994) 93; N. Sütterlin, H.J. Kurth, and G. Markert, *Makromol. Chem.* **177** (1976) 1549.
23. C. Odin, J.P. Aimé, Z. El Kaakour, and T. Bouhacina, *Surf. Sci.* **317** (1994) 321.
24. J.C. Padget and P.J. Moreland, *J. Coating Tech.* **55** (1983) 39; D.R. Stutman, A. Klein, M.S. El-Aasser, and J.W. Vanderhoff, *Ind. Eng. Chem. Prod. Res. Dev.* **24** (1985) 404.
25. E.J. Sundberg and D.C. Sundberg, *J. Appl. Polym. Sci.* **47** (1993) 1277.
26. D. Snétivy and G.J. Vancso, *Langmuir* **9** (1993) 2254.
27. C.R. Clemmer and T.P. Jr. Beebe, *Science* **251** (1991) 640.